
Gas and dust spectra of the D' type symbiotic star HD330036

R. Angeloni^{1,2}, M. Contini^{2,1}, S. Ciroti¹, and P. Rafanelli¹

¹ Dipartimento di Astronomia, Università di Padova, Vicolo dell'Osservatorio 2, I-35122 Padova, Italy rodolfo.angeloni@unipd.it, stefano.ciroti@unipd.it, piero.rafanelli@unipd.it

² School of Physics and Astronomy, Tel Aviv University, Tel Aviv 69978, Israel contini@post.tau.ac.il

Summary. We present a modelling of the D' type symbiotic star (SSs) HD330036 from radio to UV. Within a colliding-wind scenario, we analyse the continuum, line, and dust spectra by means of the SUMA code. We find that the UV lines are emitted from high-density gas downstream of the shock propagating between the stars, while the optical lines are emitted by the gas downstream of the shock propagating outwards from the system. Three shells are identified in the IR continuum SED: all of them appear to be circumbinary. Analysis of the ISO-SWS spectrum reveals that both PAHs and crystalline silicates coexist in HD330036. Strong evidence that crystalline silicates are shaped in a disk-like structure is derived on the basis of the relative crystalline band strengths.

Key words: binaries: symbiotic - stars: individual: HD330036

1 Introduction

Symbiotic systems (SSs) are interacting binaries composed of a compact star, generally a white dwarf (WD), a cool giant star, and different emitting gas and dust nebulae created by both the photoionising flux from the hot star and by collision of the winds.

Eight out of about 200 SSs known today are classified as D' types (Belczyński et al. 2000). They are characterised by a cool star of spectral type F or G which shows a significant enhancement of the s-process elements and a high rotational velocity (Zamanov et al. 2006, hereafter Z06). Moreover, these rare SSs display a significant infrared excess only beyond $\sim 3 \mu\text{m}$, suggesting a low dust temperature (Allen 1984).

D' type SSs have been classified by some authors as young, compact PN with a binary core (Lutz 1984, hereafter L84; van Winckel et al. 1994; Corradi et al. 1999) while some other ones, e.g. Schmid & Nussbaumer (1993, hereafter SN93), favour a classification of D' type systems as SSs on the basis of the ongoing interaction between the cool giant and the nebulae.

Among D' type SSs, an intriguing object is HD330036 (CN 1-1). We have modelled HD330036 (Angeloni et al. 2007a) in the light of a colliding-wind scenario. The UV and optical line spectra are analysed in §3. Subsequently, cross-checking the continuum and line ratio results, we disentangle the different emitting contributors in the spectral energy distribution (SED) in §4. We analyse the HD330036 dust features in the still unexploited ISO-SWS spectrum in §5. Discussion and concluding remarks follow in §6.

2 The colliding-wind models

Theoretical models (Kenny & Taylor 2005), as well as observations (Nussbaumer et al. 1995), have shown that in SSs both the hot and cool stars lose mass through stellar winds that collide within and outside the system, leading to a complicated structure of gas and dust nebulae. SSs can thus be treated as colliding-wind binary systems (Angeloni et al. 2007b). The calculations were performed with SUMA (Viegas & Contini 1994; Contini 1997), a numerical code that simulates the physical conditions of an emitting gaseous cloud under the coupled effect of ionisation from an external radiation source and shocks and in which both line and continuum emission from gas are calculated consistently with dust-reprocessed radiation.

3 The line spectra

We calculated the spectra by different models, m1, m2, and m3. Model m1 leads to the best fit of the calculated line ratios to those observed by L84 but, being characterised by a high V_s (300 km s^{-1}) and a high T_* (100,000 K), fails in reproducing the HeII4686/H β line ratio, as well as the FWHM profiles. Model m2 explains the line ratios observed by SN93, who derived a temperature of the hot star $T_* = 60,000$ K. Model m3 is characterised by a large a_{gr} , which is consistent with crystalline grains (see §4 and §5).

The optical spectra contain several forbidden lines that refer to relatively low critical densities for de-excitation, particularly the [OII] lines.

4 The continuum SED

The left diagram of Fig. 1 presents the modelling of the continuum SED, resulting from the contributions of the fluxes from the cool and hot stars, as well as the fluxes from the dust shells, the bremsstrahlung from the ionised nebulae downstream of the shock fronts, and the reprocessed radiation from dust. As a first guess, the flux from the stars and the dust shells is approximated by black body radiation.

4.1 The shells

The dust grain temperature is derived by modelling the ISO and IRAS data. Figure 1 (left panel) shows that the data can be explained by the combination of at least

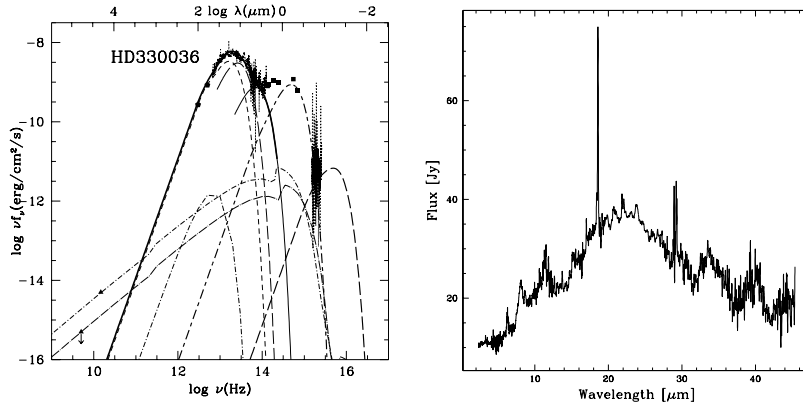


Fig. 1. Left: the SED of the continuum. The bb at 60,000K (thick long-dashed); the bb at 6000K (thick long-short dashed); the bb at 850K (thin solid); the bb at 320K (thin long-dashed); the bb at 200K (thin short-dashed); the bremsstrahlung calculated by model m2 (long-dash dot); the bremsstrahlung and relative dust emission by model m5 (short-dash dot - Angeloni et al 2007a); the summed SEDs of the dust shells (thick solid). Right: ISO-SWS spectrum of HD330036. The strongest spectral features at $\sim 18 \mu\text{m}$ and $\sim 28 \mu\text{m}$ are instrumental artifacts. Notice the bands usually attributed to polycyclic aromatic hydrocarbons PAHs (at 3.3, 6.2, 8, and 11.3 μm). At longer wavelengths we found evidence of emission from crystalline silicates, clearly visible in the strong complexes at $\sim 33 \mu\text{m}$ and $\sim 40 \mu\text{m}$.

three black body (bb) fluxes, corresponding to temperatures of 850 K, 320 K, and 200 K. By comparing the models with the data we are able to calculate the dust shell radii, once adopted a distance to the Earth $d=2.3$ kpc: we find $r= 2.8 \cdot 10^{13}$ cm, $4 \cdot 10^{14}$ cm, and 10^{15} cm for the shells at 850 K, 320 K, and 200 K, respectively. Interestingly, this implies that all the dust shells are circumbinary if we assume an upper limit for binary separation of $\sim 8 \cdot 10^{12}$ cm ($5 R_g$), as suggested by Z06.

4.2 The shocked nebulae

The continua, calculated by the models and cross-checked by the line ratios, were compared with the observations in Fig. 1. We have found that the physical parameters that best explain the shocked nebulae are $T_*=60000\text{K}$, $V_s=150 \text{ km s}^{-1}$, $n_0=4 \cdot 10^7 \text{ cm}^{-3}$, $a_{gr}=0.2 \mu\text{m}$ for the reverse shock, while for the expanding shock we found $V_s=50\text{km s}^{-1}$, $n_0=1.5 \cdot 10^5 \text{ cm}^{-3}$ and grains of both sizes, $a_{gr}=0.2 \mu\text{m}$ and $2 \mu\text{m}$.

5 The solid state features in the ISO spectrum

The ISO-SWS spectrum of HD330036 can be clearly split into two regions: the short wavelength one (up to $\sim 15 \mu\text{m}$) dominated by PAH prominent emission bands and the long one showing a blending of narrow and characteristic emission profiles, whose carriers are believed to be crystalline silicates.

5.1 PAHs

HD330036 exhibits some strong emission bands at 3.3, 6.2, 7.7, 8.6, and 11.3 μm : the so-called unidentified infrared (UIR) emission features (Puget & Leger 1989; Allamandola et al. 1989), generally attributed to PAHs, or to small grains containing PAHs. A careful profile analysis of these bands suggests that PAHs lay in the inner region ($T \sim 850\text{K}$, $r \sim 2.8 \cdot 10^{13}$ cm) of the HD330036 system.

5.2 Crystalline silicates

The ISO-SWS spectrum beyond $\sim 15 \mu\text{m}$ shows the bands usually attributed to crystalline silicates.

Several studies have pointed out that the high abundance of crystalline silicate may be related to the geometry of dust distribution. The analysis of the crystalline silicate bands in HD330036 (in particular, of the olivine ones) suggests a disk-like geometry of the silicate envelope.

A further constraint on the temperature, based on the relative strength ratio of the forsterite bands, along with the disk geometry deduced above, might indicate that the crystalline silicates in HD330036 reside in the outer large circumbinary envelopes of dust that were found by modelling the IR SED in §4.

It has been proposed (Harker & Desch 2002) that shocks might play a non secondary role in the dust crystallisation processes. Our models show that crystallisation processes in HD330036 may be triggered by shocks and that annealing may take place within the circumbinary disk.

6 Discussion and concluding remarks

The analysis of the D' type SS HD330036 has been presented by modelling the continuum SED, along with the line and dust spectra within a colliding-wind binary scenario (Angeloni et al. 2007a).

We have found that the UV lines are emitted from high-density gas between the stars downstream of the reverse shock, while the optical lines are emitted downstream of the shock propagating outwards the system. The models that best explain both the observed UV and optical line ratios correspond to $T_* = 60,000\text{K}$: regarding the gas density, in the downstream region of the reverse shock it reaches 10^8 cm^{-3} , while it is $\sim 10^6 \text{ cm}^{-3}$ downstream of the expanding shock.

The SED of the continuum has been disentangled in the different gas and dust contributions. Three shells are identified in the continuum IR SED: interestingly, all these shells appear to be circumbinary.

The analysis of the ISO-SWS spectrum has revealed that both PAHs and crystalline silicates coexist in HD330036, with PAHs associated with the internal, hotter shell, and crystalline silicates stored in the cooler and outer disk-like structure.

The proposed scenario would link HD330036 to some bipolar Post-AGB stars that have shown this sort of dichotomy in the dust composition, location, and geometrical distribution (Molster et al. 2001, Matsuura et al. 2004).

Finally, we suggest that the crystallisation processes in HD330036 may be triggered by shocks and that annealing may take place within the circumbinary disk.

The VLTI/MIDI observations (P.I. D'Onofrio - 079.D-0242) based on the model we presented and recently performed by ESO aims to unveil the HD330036 dust environment by means of IR interferometric observations.

References

1. Allamandola, L. J., Tielens, G. G. M., & Barker, J. R. 1989, *ApJS*, 71, 733
2. Allen, A. 1984, *Ap&SS*, 99, 101
3. Angeloni, R., Contini, M., Ciroi, S., Rafanelli, P. 2007a, *A&A*, accepted for publication
4. Angeloni, R., Contini, M., Ciroi, S., & Rafanelli, P. 2007b, *AJ*, 134, 205
5. Belczyński, K., Mikołajewska, J., Munari, U., Ivison, R. J., & Friedjung, M. 2000, *A&Ap Suppl. Ser.*, 146, 407
6. Contini, M. 1997, *ApJ*, 483, 887
7. Corradi, R. L. M., Brandi, E., Ferrer, O. E., & Schwarz, H. E. 1999, *A&A*, 343, 841
8. Harker, D. E., & Desch, S. J. 2002, *ApJ*, 565, L109
9. Kenny, H. T., & Taylor, A. R. 2005, *ApJ*, 619, 527
10. Lutz, J.H. 1984, *ApJ*, 279, 714
11. Matsuura, M., et al. 2004, *ApJ*, 604, 791
12. Molster, F. J., Yamamura, I., Waters, L. B. F., Nyman, L.-Å., Käuffl, H.-U., de Jong, T., & Loup, C. 2001, *A&A*, 366, 923
13. Nussbaumer, H., Schmutz, W., & Vogel, M. 1995, *A&A*, 293, L13
14. Puget, J. L., & Leger, A. 1989, *ARA&A*, 27, 161
15. Schmid, H. M., & Nussbaumer, H. 1993, *A&A*, 268, 159
16. Van Winckel, H., Schwarz, H. E., Duerbeck, H. W., & Fuhrmann, B. 1994, *A&A*, 285, 241
17. Viegas, S. M., & Contini, M. 1994, *ApJ*, 428, 113
18. Zamanov, R. K., Bode, M. F., Melo, C. H. F., Porter, J., Gomboc, A., & Konstantinova-Antova, R. 2006, *MNRAS*, 365, 1215